CHARM PRODUCTION
AT THRESHOLD

(DRAFT 08/06/00)

1 General motivations

The threshold regime of charmonium and open charm production opens up a new window into QCD dynamics, particularly multiquark, gluonic and hidden color correlations in nucleons and nuclei. In contrast to diffractive charm production at high energy which tests the behavior of the gluon structure functions at small x, charm production near threshold tests the structure of the target near $x = 1$ and its short range behavior.

This has to do with the kinematics of the reaction products. For J/ψ production on nucleon, the threshold energy is $E_\gamma = 8.20$ GeV and, due to the large mass of the charmed quark ($m_c \approx 1.5$ GeV), the $c\bar{c}$ fluctuation of the photon travels over $l_c \cong 2E_\gamma/4m_c^2 = .36$ fm (see Fig. 1). The large mass of the charmed quark imposes also a small transverse size $r_\perp \sim 1/m_c = 0.13$ fm of this fluctuation. The minimum value allowed for the momentum transfer is large ($t_{min} \sim 1.7$ GeV^2 at the very threshold, ~ 1 GeV^2 at $E_\gamma = 10$ GeV). Thus charm production near threshold implies a small impact parameter ($b \sim 1/\sqrt{-t} \sim 0.2$ fm). All the five valence quarks (the two heavy charm quarks in the probe and the three light quarks in the target) must be in the same small interaction volume.

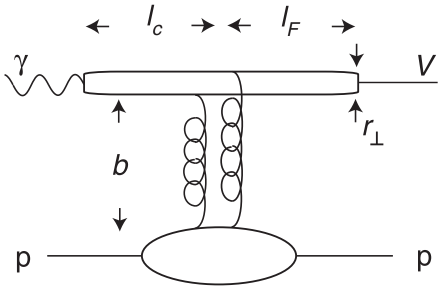

Figure 1: The characteristic time scales in J/ψ production on proton.

Consequently, all the quarks must be involved in the reaction mechanism. On nucleon targets, this implies that three gluon exchange may take over two gluon and one gluon exchange, and open the way to the study of correlations between valence quarks. On few body targets, each exchanged gluon may couple to a colored quark cluster and reveal the hidden color part of the nuclear wave function, a domain of short range nuclear physics where nucleons lose their identity. Such exotic configurations are more likely to appear below the threshold for charm creation on a nucleon at rest, where quasi free production is suppressed. On deuterium the threshold for J/ψ production is ~ 5.65 GeV, while on heavy nuclei the threshold is simply the J/ψ mass 3.1 GeV.

At threshold, the formation length (during which the $c\bar{c}$ pair evolves into a J/ψ, after its interaction with a nucleon)

$$l_F \cong \frac{2}{m_{\psi'} - m_{J/\psi}} \left[\frac{E_{J/\psi}}{2m_c}\right] \cong 0.11 E_\gamma \tag{1}$$

is around 1 fm, closer to the nucleon size than the nucleus size. This is the ideal situation to determine the scattering cross section of a full sized charmed meson on a nucleon, contrary to higher energies which rather give access to the nuclear interaction of a compact $c\bar{c}$ pair. Besides its own interest, this may be a useful input in the studies of QGP.

Finally, intrinsic charm components in the proton ground state and possible penta-quark resonances or charmonium bound states may be revealed near threshold. The discovery of such qualitatively new states of matter would be a major success for CEBAF12.

Since no quantitative predictions exist for charm production near threshold, we will rely on interesting conjectures on the short distance behavior of hadronic matter, inferred from properties of perturbative QCD. Experiments are mandatory to explore this virgin frontier of our knowledge.

2 Nucleon

2.1 Higher Twist Effects

At high energy the dominant contribution to hard processes comes from "leading twist" diagrams, characterized by only one parton from each colliding particle participating in the large momentum (Q) subprocess. Since the time scale of the hard collision is $1/Q$, only partons within this transverse distance can affect the process. The likelihood that two partons are found so close to each other is typically proportional to the transverse area $1/Q^2$ and leads to the suppression of higher twist, multiparton contributions.

In contrast, higher twist effects are enhanced close to the kinematical boundary. For example, in the $\gamma p \to c\bar{c}p$ reaction near threshold, all the partons have to transfer their energy to the charm quarks within their proper creation time $1/m_c$, and must be within this transverse distance from the $c\bar{c}$ and from each other. Hence only compact proton Fock states, with a radius equal to the compton wavelength of the heavy quark, can contribute to charm production at threshold.

The effective proton radius in charm photoproduction near threshold can be inferred from the following argument [1, 2]. As indicated in Fig. 2a, one mechanism is that most of the proton momentum is first transferred to one (valence) quark, followed by a hard subprocess $\gamma q \to c\bar{c}q$. If the photon energy is $E_\gamma = \zeta E_\gamma^{th}$, where E_γ^{th} is the energy at kinematic threshold ($\zeta \geq 1$), the valence quark must carry a fraction $x = 1/\zeta$ of the proton (light-cone) momentum. The lifetime of such a Fock state (in the light-cone or infinite momentum frame) is $\tau = 1/\Delta E$, where

$$\Delta E = \frac{1}{2p}\left[m_p^2 - \sum_i \frac{p_{i\perp}^2 + m_i^2}{x_i}\right] \simeq \frac{\Lambda_{QCD}^2}{2p(1-x)} \tag{2}$$

For $x = 1/\zeta$ close to unity such a short lived fluctuation can be created (as indicated in Fig. 2a) through momentum transfers from valence states (where the momentum is divided

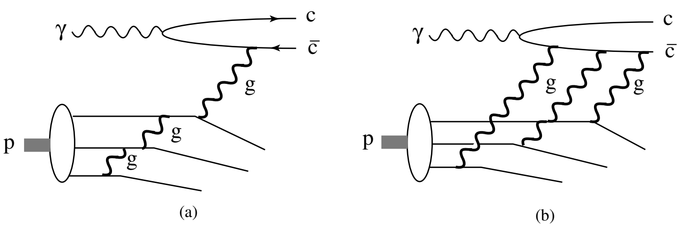

Figure 2: Two mechanisms for transferring most of the proton momentum to the charm quark pair in $\gamma p \to c\bar{c}p$ near threshold. The leading twist contribution (a) dominates at high energies, but becomes comparable to the higher twist contribution (b) close to threshold (adapted from Fig. 9 of Ref. [1]).

evenly) having commensurate lifetimes τ and transverse extension

$$r_\perp^2 \simeq \frac{1}{p_\perp^2} \simeq \frac{\zeta - 1}{\Lambda_{QCD}^2} \tag{3}$$

This effective proton size thus decreases towards threshold ($\zeta \to 1$), reaching $r_\perp^2 \simeq 1/m_c^2$ at threshold ($\zeta - 1 \simeq \Lambda_{QCD}^2/m_c^2$).

As the lifetimes of the contributing Fock states approach the time scale of the $c\bar{c}$ creation process, the time ordering of the gluon exchanges implied by Fig. 2a ceases to dominate higher twist contributions such as that of Fig. 2b [2]. There are in fact reasons to expect that the latter diagrams give a dominant contribution to charmonium production near threshold. First, there are many more such diagrams. Second, they allow the final state proton to have a small transverse momentum (the gluons need $p_\perp \simeq m_c$ to couple effectively to the $c\bar{c}$ pair, yet the overall transfer can still be small in Fig. 2b). Third, with several gluons coupling to the charm quark pair its quantum numbers can match those of a given charmonium state without extra gluon emission.

The above discussion is generic, and does not indicate how close to threshold the new effects actually manifest themselves. While more quantitative model calculations certainly are called for, this question can only be settled by experiment. It is desirable to measure both the cross section and polarization for several charmonium states, as well as for open charm.

2.2 A Model for the Cross Section near Threshold

In order to estimate the counting rate of charm production near threshold we will rely on a simple model.

Near threshold charm production probes the $x \simeq 1$ configuration in the target, the spectator partons carrying a vanishing fraction $x \simeq 0$ of the target momentum. This implies that the production rate behaves near $x \to 1$ as $(1-x)^{2n_s}$ where n_s is the number of spectators. Perturbative QCD predicts three different gluonic components of the photoproduction cross-section:

- The usual one gluon $(1-x)^4$ distribution for leading twist photon-gluon fusion $\gamma g \to c\bar{c}$, which leaves two quarks spectators;

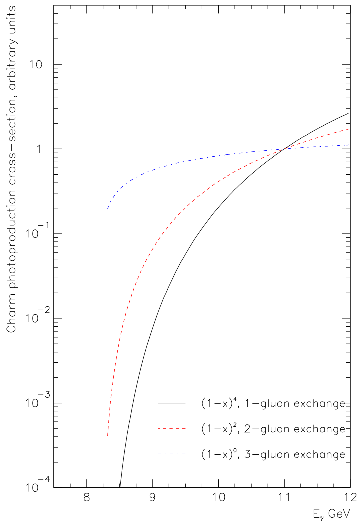

Figure 3: Variation of the cross sections of various mechanisms for charm production near threshold.

- Two correlated gluons emitted from the proton with a net distribution $\frac{(1-x)^2}{R^2\mathcal{M}^2}$ for $\gamma gg \to c\bar{c}$, leaving one quark spectator;
- Three correlated gluons emitted from the proton with a net distribution $\frac{(1-x)^0}{R^4\mathcal{M}^4}$ for $\gamma ggg \to c\bar{c}$, leaving no quark spectators.

Here $x \approx (2m\mathcal{M} + \mathcal{M}^2)/(s - m^2)$ and $\mathcal{M}$ is the mass of the $c\bar{c}$ pair. The relative weight of the multiply connected terms is controlled by the interquark separation $R \simeq 1/m_c$. The extra powers of $1/\mathcal{M}$ arise from the higher twist hard processes (see Ref. [3]).

Such a behavior is schematically depicted in Fig. 3. The two gluon term produces odd C quarkonium $\gamma gg \to J/\psi$, thus permitting exclusive $\gamma p \to J/\psi p$ production. The photon three-gluon coupling $\gamma ggg \to c\bar{c}$ produces a roughly constant term at threshold in σ/v, where it is expected to dominate (here $v = 1/16\pi(s - m^2)^2$ is the usual phase space factor). It produces the $\eta_c p$, $\chi_c p$ and other C even resonances, but also J/ψ. Indeed, there is evidence [4] that the J/ψ elastic photoproduction cross section is roughly flat up to $E_\gamma \approx 12$ GeV, as depicted in Fig. 4, contrary to the steep variation at higher energies.

For elastic charm production (when the proton target remains bound), it is also necessary to take into account the recombination of the three valence quarks into the proton via its form factor, as well as the coupling of the photon to the $c\bar{c}$ pair. For two gluon exchange the cross section of the $\gamma p \to J/\psi p$ takes the form:

$$\frac{d\sigma}{dt} = \mathcal{N}_{2g} v \frac{(1-x)^2}{R^2\mathcal{M}^2} F_1(\frac{t}{4})(s - m^2)^2 \tag{4}$$

while for three gluon exchange it takes the form:

$$\frac{d\sigma}{dt} = \mathcal{N}_{3g} v \frac{(1-x)^0}{R^4\mathcal{M}^4} F_1(\frac{t}{9})(s - m^2)^2 \tag{5}$$

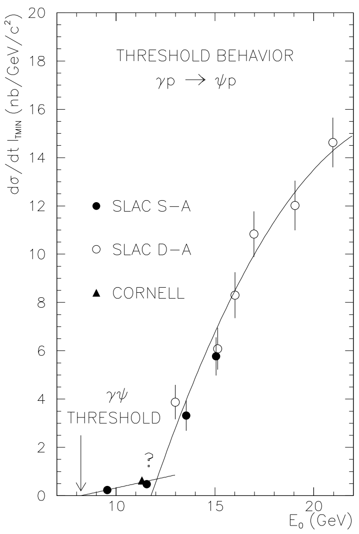

Figure 4: The cross section measured at t_{min}, at SLAC [5] and Cornell [6] in two arm experiments, and SLAC [4] in one arm experiment.

where $F_1(t)$ is the isoscalar proton form factor. Its argument takes into account that the momentum transfer is shared between two or three valence quarks in the proton. This implies that the t distribution for the three gluon exchange cross section is flatter than for two gluon exchange cross section. The $(s - m^2)^2$ term comes from the coupling of the incoming photon to the $c\bar{c}$ pair (see, for instance, Ref. [7]) and compensates the same term in the phase space v.

The normalization coefficient $\mathcal{N}$ is determined assuming that each channel saturates the experimental cross section measured at Cornell [6] around $E_\gamma = 12$ GeV.

Note that such expressions are valid in limited energy range near threshold, where $x \sim 1$. At higher energies, one has to rely on the variation of the gluon distribution in the vicinity of $x \sim 0$ to reproduce the step rise of charm photoproduction [8, 9].

In addition, possible penta-quark resonances in the s-channel may modify this picture as schematically depicted in Fig. 5. Also Final State Interactions (FSI) may affect these predictions, but it is very likely that the trend of the cross-sections will remain unchanged (near threshold their differ by orders of magnitude). Only experiments can answer these open questions, and the proposed cross sections should be considered as an educated guess for a feasibility study.

3 Nuclei

3.1 Subthreshold Photoproduction

The high luminosity of CEBAF12 will allow detailed study of subthreshold production of charm(onium). It is well established that antiprotons and kaons (and even anti-deuteron) are produced on nuclear target at substantially lower energies than is kinematically possible on free nucleons [10]. Scattering on a single nucleon in the nucleus would at these energies require

Figure 5: A possible signal of a s-channel resonance, on top of the three gluon contribution.

Figure 6: Two conceptual mechanisms for subthreshold $\overline{p}$ in hA collisions. In (a) the production occurs locally off a hot spot (black circle) of high energy density in the nucleus. In (b) the light quarks gain momentum over an extended nuclear region (grey).

a Fermi momentum in the vicinity of 800 MeV/c. While the pA data can be fit assuming such high Fermi momenta, this assumption leads to an underestimate of subthreshold production in AA collisions by about three orders of magnitude [11].

There are at least two qualitatively different scenarios for the observed subthreshold production of antiprotons [1]. Either (Fig. 6a) the projectile strikes a local "hot spot" with a high energy density in the nucleus. The effective mass of the scatterer is high, lowering the kinematical threshold. Alternatively (Fig. 6b) the momentum required to create the anti proton is not transferred locally, but picked up in an extended longitudinal region: the nucleus plays the role of a "femtoaccelerator". Establishing either scenario would teach us something qualitatively new about rare, highly excited modes of the nucleus.

Photoproduction of charm below threshold would be of crucial help in distinguishing the correct mechanism, at least for the two following reasons:

- The $c\overline{c}$ component of the photon is almost point like at the charm threshold and below. In particular, effects due to the shrinking effective size of the hadron probe near threshold are eliminated;

- The $c\overline{c}$ pair is created locally, within a proper time $\tau \simeq 1/m_c$. The extended acceleration scenario of Fig. 6b is thus not effective for charm photoproduction. If significant subthreshold charm photoproduction occurs (beyond what can be ascribed to standard Fermi motion) this selects the hot spot scenario of Fig. 6a.

3.2 Interaction of $c\overline{c}$ Pairs in Nuclei

Close to threshold for the process $\gamma p \to J/\psi p$ on stationary protons the energy of the J/ψ is $E_{J/\psi} \simeq 7$ GeV. This corresponds to a moderate Lorentz γ factor $E_{J/\psi}/M_{J/\psi} \simeq 2.3$. Hence a

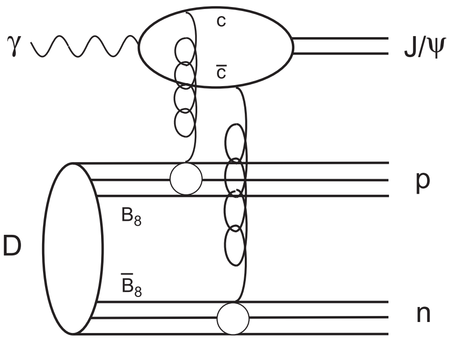

Figure 7: The simplest diagram to reveal hidden color state in deuterium [16].

significant expansion of the $c\overline{c}$ pair occurs inside a large nucleus, and effects of charmonium bound states in nuclei may be explored.

The dependence of the ratio $\sigma(J/\psi)/\sigma(D\overline{D})$, between hidden and open charm production, on the target size A and on the projectile energy indicates the amount of rescattering in the nucleus. The presently available data on the A-dependence of charmonium production is at much higher energies, and thus measures the nuclear interactions of a compact $c\overline{c}$ pair rather than of the full sized charmonium. Further information about the significance of the radius of the charmonium state can be obtained by comparing ψ' to J/ψ production on various nuclei. In high energy hA and γA scattering both states have similar A-dependence [12].

Information about the propagation of charmonium in nuclei is also very important for relativistic heavy ion collisions, where charmonium production may be a signal for quark-gluon plasma formation. Charmonium photoproduction near threshold provides us with the unique possibility to study the propagation of a full fledged charmonium state in cold hadronic matter.

Even though the $c\overline{c}$ pair is created with rather high momentum at threshold, it may be possible to observe reactions where the pair is captured by the target nucleus, forming "nuclear-bound quarkonium" [13]. This process should be enhanced in subthreshold reactions. There is no Pauli blocking for charm quarks in nuclei, and it has been estimated that there is a large attractive Van der Waals potential binding the pair to the nucleus [14].

3.3 Hidden Color Configurations

The existence of such hidden color configurations are predicted by QCD evolution equations [15]. It is striking that in $\gamma d \to J/\psi pn$ the $|8_c 8_c>$ hidden color state of the deuteron couples so naturally by two gluons to the $J/\psi pn$ final state [16]. Such a contribution may dominate subthreshold production, since the high momentum of the nucleon suppresses quasi free mechanisms. It may imply the detection of one of the nucleons.

When the nucleon is embedded in the nuclear medium, two mechanisms govern the photo- and the electroproduction of J/ψ mesons. The first is trivial: it is the quasi-free production mechanism. The second is much more interesting. It is the exchange of two gluons, each of them coupled to a quark belonging to a different nucleon (Fig. 7). Since the coupling of a single gluon to a quark changes its color, two gluon exchange provides us with a way to look for hidden color components, or more generally for the correlation between two quarks in hadronic matter. A coincidence experiment, for instance $D(\gamma, J/\psi p)n$ or $^3He(\gamma, J/\psi 2p)n$, must be performed to disentangle them.

The cross section of the quasi-free process in the $D(\gamma, J/\psi p)n$ reaction takes the form [17]:

$$\frac{d\sigma}{dtd\vec{n}} = (1 \; + \; \beta_n \cos\theta_n) \left. \frac{d\sigma}{dt} \right|_{\gamma p \to J/\psi p} \rho(\mid \vec{n} \mid) \tag{6}$$

where $\mid \vec{n} \mid$, θ_n and β_n are respectively the momentum, the polar angle and the velocity of the spectator neutron, and where $\rho(\mid \vec{n} \mid)$ is nothing but the nucleon momentum distribution in deuterium. When integrated against the angles of the spectator neutron, this expression reduces to:

$$\frac{d\sigma}{dtd\mid \vec{n} \mid} = \left. \frac{d\sigma}{dt} \right|_{\gamma p \to J/\psi p} 4\pi \vec{n}^2 \rho(\mid \vec{n} \mid) \tag{7}$$

with $\int \rho(\mid \vec{n} \mid) d\vec{n} = 1$.

It decreases very quickly [17] as the undetected neutron momentum increases. Consequently, selecting high values of neutron momentum is the way to suppress the contribution from such a trivial mechanism. The quasi-free contribution in Fig. 8 has been computed with the Paris wave function [18] of the deuterium.

The cross section corresponding to the exchange of each of the two gluons with a different quark cluster is expected to exhibit a flatter momentum distribution, since the recoil momentum is shared between the two nucleons. However it is very difficult to make a reliable quantitative estimate of its magnitude.

A rough, approach would be to write the corresponding cross section as :

$$\frac{d\sigma}{dtd\mid \vec{n} \mid} = \left. \frac{d\sigma}{dt} \right|_{\gamma p \to J/\psi p} 4\pi \vec{n}^2 \left[\varphi_{cc}(\frac{\vec{n}}{2}) \right]^2 \frac{F_1^4(\frac{t}{4})}{F_1^2(t)} \tag{8}$$

where the fourth power of the nucleon form factor comes from the fact that two nucleons have to recombine, each at the momentum transfer $t/4$. It is assumed that the form factor of the transition between a colored cluster and the nucleon does not differ too much from the nucleon form factor. The ratio of the nucleon form factors acts as an enhancement factor $\simeq 7$ at $-t = 1 \; GeV^2$, for example. It is also assumed that the recoil momentum is equally shared between the two colored clusters whose wave function is $\varphi_{cc}(\frac{\vec{n}}{2})$. This component of the deuterium wave function is unknown, and only few predictions are available. As an example and to set the order of magnitude, the hidden color contribution in Fig. 8 has been obtained by using the Fourier transform of the wave function depicted in Fig. 11 of Ref. [19]. Since it exhibits a node around 500 MeV/c, a node appears in the cross-section around $n \simeq 1 \; GeV/c$. This is unphysical, since in a more elaborate calculation the integration against the nucleon internal momentum washes it out. Anyway, this rough estimate shows that the hidden color component contribution dominates the cross-section above 0.5 GeV/c. The calculation reported in [19] predicts a probability of finding a hidden color component in the deuterium wave function of the order of 0.1%. Fig. 8 also shows what one may expect for a probability around 1%.

In order to increase the probability of the hidden color component, or to enhance the effect of correlations between quarks, one would like to increase the density of the target nucleus.

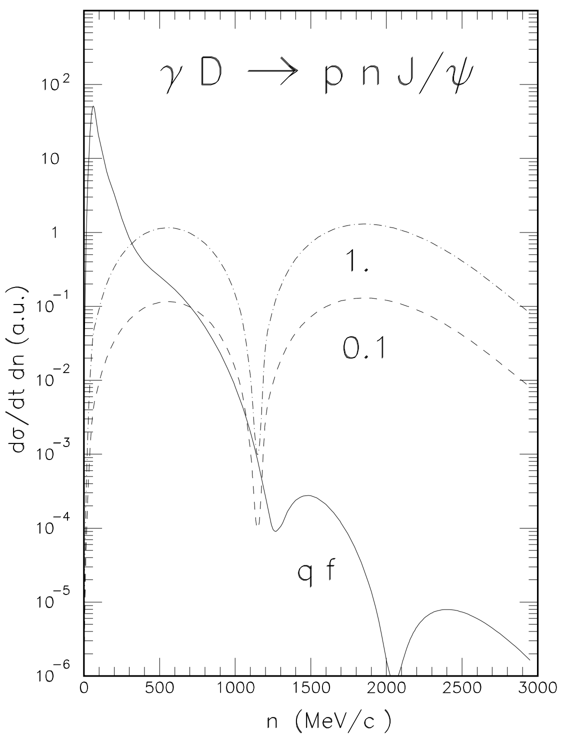

Figure 8: The variation of the cross-section of the reaction $\gamma D \to pnJ/\psi$ against the neutron momentum $|\vec{n}|$, at fixed t. Solid line: quasi-free contribution. Dashed line: contribution of hidden color component when its probability is 0.1%. Dash-dotted curve: the same for a probability of 1%

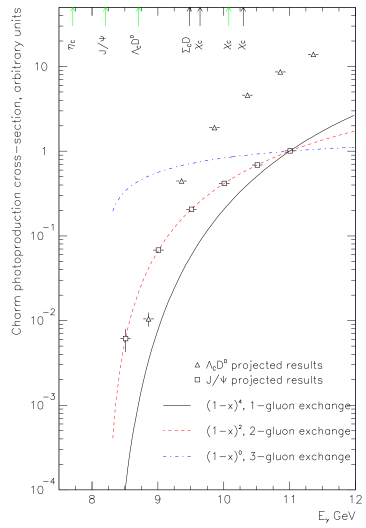

Figure 9: Counting rate for various mechanisms of charm production near threshold.

The reactions ${}^3He(\gamma, J/\psi 2p)n$ and ${}^4He(\gamma, J/\psi 2p)nn$ are good candidates. A further advantage comes from the fact that the target pp pair is almost in a pure ${}^1S_0$ state (see for instance [20]), contrary to the deuterium which has a sizable D wave component. The high momentum tail of the quasi-free process is reduced accordingly, leaving more room for two gluon exchange quark rearrangement processes.

4 Reactions Accessible at CEBAF12

The high luminosity at CEBAF12 will open the way to the determination of the cross section of selected channels on nucleon and few nucleon targets. We have chosen to study the feasibility of reactions where the charmed particle is identified by its charged decay products.

4.1 Elastic Charmonium Photoproduction: $\gamma p \to J/\psi p$

J/Ψ elastic production on nucleon and quasi elastic production on nuclei, are identified by the detection of e^+e^- pairs in a segmented calorimeter. The detection of the recoiling proton may ease the channel identification, especially in nuclei.

The counting rate estimate (Fig. 9) indicates a pretty good distinction between the two and three gluon exchange hypothesis.

4.2 Open Charm Photoproduction

The channel $\gamma p \to p\Lambda_c D_0$ is identified by the $D_0 \to K^+\pi^-$ decay, using two magnetic spectrometers. As shown in Fig. 9, the counting rate is high even near threshold.

4.3 Charm production in Few Nucleon Systems

Assuming that the three gluon exchange dominates at threshold and below, the energy dependence of the elementary charm production process is constant and the energy variation of the integrated cross-section of the reaction $\gamma D \to pnJ/\psi$ below threshold is driven by the recoil neutron minimum momentum n_{min} and the minimum four-momentum t_{min}:

$$\sigma(E_\gamma) \propto \int_{n_{min}}^{n_{max}} \int_{t_{max}}^{t_{min}} \frac{d\sigma}{dtd|\,\vec{n}\,|} dtd|\,\vec{n}\,| \tag{9}$$

The dependence upon t_{min} is the same, or very similar, for the quasi-free and the hidden color contributions: in both cases it is controlled by the nucleon form factor. On the contrary, their dependence upon n_{min} is quite different. As the photon energy E_γ decreases below threshold, the allowed minimum momentum of the recoil neutron increases: as it can be inferred from Fig. 8, the quasi-free contribution is suppressed as $\rho(n_{min})$, in contrast to the hidden color contribution which is roughly constant and depends slowly on the value of (n_{min}).

(*I will work out the corresponding numerics, beginning of June*)

(*Insert here a Figure showing the expected counting rate against the energy below threshold.*)

5 A dedicated apparatus

6 Hall D opportunities

7 Conclusions

Charm production near threshold has remarkable sensitivity to new physics, not only the target proton or nuclei, but also the charm system itself. All of the valence quarks of the target are forced to act as a coherent compact state in order that all of the available energy be focused into heavy flavor production. In the case of nuclear targets, charm production in the subthreshold regime is sensitive to hidden-color non-nucleonic correlated states, Fock components which must occur according to QCD evolution equations. The unpublished data from SLAC on J/ψ production near threshold appears to be remarkably flat, indicating that such high correlated mechanisms may indeed be relevant. We have also noted that the production of charmonium states of even and odd C can selectively reveal different coherent mechanisms at threshold. On the other hand the production of charm states at low relative velocity in the target allows the study of the QCD van der Waals interaction and the production of exotic charm resonances or bound states, such as the penta-quark or nuclear bound quarkonium.

We have performed a feasibility study for two options: a dedicated detector and the facility foreseen in Hall D.

to be completed...

References

[1] P. Hoyer, Nucl. Phys. A622 (1997) 284c.

[2] S.J. Brodsky, et al. Nucl. Phys. B369 (1992) 519.

[3] E.L. Berger and S.J. Brodsky, Phys. Rev. Lett. 42 (1979) 940.

[4] R. Anderson et al., SLAC-PUB-1741 *Invited talk presented at Int. Conf. on Production of Particles with New Quantum Numbers, Wisconsin U., Madison, Apr. 22-24, 1976.*

[5] R. Anderson et al., Phys. Rev. Lett. 38 (1977) 263.

[6] B. Gittelman et al., Phys. Rev. Lett. 35 (1975) 1616.

[7] J.M. Laget, preprint hep-ph/0003213, March 2000.

[8] S.J. Brodsky et al., Phys. Rev. D50 (1994) 3194.

[9] D. Kharzeev et al., hep-ph/9901375 (Jan. 1999).

[10] J.B. Carroll et al., Phys. ReV. Lett. 62 (1989) 1829;
A. Shor et al., Phys. Rev. Lett. 63 (1989) 2193;
A. Schröter et al, Z. Phys. A350 (1994) 101.

[11] A. Shor et al., Nucl. Phys. A514 (1990) 717.

[12] J. Badier et al., Z. Phys. C20 (1983) 101;
S. Katsanevas et al., Phys. Rev. Lett. 60 (1988) 2121;
D.M. Alde et al., Phys. Rev. Lett. 66 (1991) 133 and 2285;
M.J. Leitch et al., Nucl. Phys. A544 (1992) 197c.

[13] S.J. Brodsky, G.F. de Teramond and I.A. Schmidt, Phys. Rev. Lett. 64 (1990) 1924.

[14] M. Luke, A.V. Manohar and M.J. Savage, Phys. Lett. B288 (1992) 355.

[15] S. J. Brodsky, C. Ji and G. P. Lepage, Phys. Rev. Lett. 51 (1983) 83.

[16] J.M. Laget and R. Mendez-Galain, Nucl. Phys. **A581** (1995) 397.

[17] J.M. Laget, Phys. Rep. 69 (1981) 1.

[18] M. Lacombe *et al., Phys. Lett.* **B101** (1981) 139.

[19] Y. Yamauchi and Wakamatsu, *Nucl. Phys.* **A457** (1986) 621.

[20] C. Hajduk and P.U. Sauer, *Nucl. Phys.* **A369** (1981) 321.